Site-Specific Effects of Compression on Macromolecular Diffusion in Articular Cartilage

Holly A. Leddy and Farshid Guilak
Department of Surgery and Department of Biomedical Engineering, Duke University Medical Center, Durham, North Carolina 27710

ABSTRACT Articular cartilage is the connective tissue that lines joints and provides a smooth surface for joint motion. Because cartilage is avascular, molecular transport occurs primarily via diffusion or convection, and cartilage matrix structure and composition may affect diffusive transport. Because of the inhomogeneous compressive properties of articular cartilage, we hypothesized that compression would decrease macromolecular diffusivity and increase diffusional anisotropy in a site-specific manner that depends on local tissue strain. We used two fluorescence photobleaching methods, scanning microphotolysis and fluorescence imaging of continuous point photobleaching, to measure diffusion coefficients and diffusional anisotropy of 70 kDa dextran in cartilage during compression, and measured local tissue strain using texture correlation. For every 10% increase in normal strain, the fractional change in diffusivity decreased by 0.16 in all zones, and diffusional anisotropy increased 1.1-fold in the surface zone and 1.04-fold in the middle zone, and did not change in the deep zone. These results indicate that inhomogeneity in matrix structure and composition may significantly affect local diffusive transport in cartilage, particularly in response to mechanical loading. Our findings suggest that high strains in the surface zone significantly decrease diffusivity and increase anisotropy, which may decrease transport between cartilage and synovial fluid during compression.

INTRODUCTION

Articular cartilage is an avascular and alymphatic tissue, in which diffusion serves as the primary mode of transport for nutrients, oxygen, waste products, signaling molecules, and matrix macromolecules. Understanding the factors that influence diffusive transport in cartilage is important for an understanding of normal cartilage function, and in the development of engineered tissue replacements (1–6). Previous studies showed that the diffusion of solutes in cartilage is dependent on a number of factors, including the size, structure, and charge of the solute, the composition and structure of the tissue, and the mechanical load on the extracellular matrix. For example, static compression decreases the diffusivity of solutes in cartilage as a function of the molecular weight of the molecule, with the greatest effects on the largest solutes (7–9). The application of a static load to cartilage was shown to decrease biosynthesis, and it was hypothesized that this decrease may be attributable, in part, to the decreased transport of nutrients to the chondrocytes (10–12).

In cartilage explants, the decrease in diffusivity was shown to be a function of the compressive strain applied to tissue explants (7–9). However, in mature articular cartilage, compression causes nonuniform strains and matrix reorganization with depth from the tissue surface (i.e., the surface, middle, and deep zones), because of the differences in proteoglycan content and collagen structure and content among different zones (13–15). Not only does compression cause closer packing of the matrix macromolecules within cartilage because of exudation of the interstitial water, but it also causes reorientation of those molecules in a manner that can affect the anisotropy of tissue properties such as permeability (16,17). Micromagnetic resonance imaging (18) and scanning electron microscopy (19) studies of the collagen structure of cartilage showed that compression causes the middle-zone collagen, which is normally randomly oriented, to become oriented more parallel to the surface. The parallel collagen structure of the surface zone was associated with the diffusional anisotropy of large molecules (20), where diffusion along fibers occurs faster than diffusion perpendicular to fibers. Because diffusional anisotropy is a function of the fiber volume fraction (21,22), compression should increase the fiber volume fraction, and therefore increase diffusional anisotropy.

This study examined the hypothesis that compression of articular cartilage decreases the diffusivity of solutes in the extracellular matrix in a site-specific manner because of the zonal differences in the structure and properties of the tissue. Furthermore, we hypothesized that compression will increase diffusional anisotropy in a manner that correlates with the magnitude of local tissue strain. These hypotheses were tested by measuring the diffusion coefficients and diffusional anisotropy of a neutral fluorescent dextran solute in a site-specific manner, and by correlating these properties with the local magnitudes of compressive and dilatational strains at various depths measured using texture correlation analysis.

METHODS

Measurement of diffusion coefficients

Full-thickness explants (1 mm thick, and 5 mm wide) of articular cartilage with 3 mm of bone attached were harvested from porcine femoral condyles.

Submitted May 16, 2008, and accepted for publication July 21, 2008.

Address reprint requests to Farshid Guilak, Dept. of Biomedical Engineering, 375 MSRB, Box 3093, Duke University Medical Center, Durham, NC 27710. Tel.: 919-684-2521; Fax: 919-681-8490; E-mail: guilak@duke.edu.

Editor: Jason M. Haugh.

0006-3495/08/11/4890/06 $2.00

doi: 10.1529/biophysj.108.137752

Explants were incubated for 4 h in Syto-64 (Molecular Probes, Eugene, OR) to label cell nuclei, and for 24 h in 70 kDa fluorescein isothiocyanate-conjugated dextran. Tissue was placed in a custom-built device with stainless-steel platens attached to a micrometer, allowing application of a prescribed static deformation (23,24). The bottom of the device consists of a coverslip, so that tissue can be imaged with a confocal microscope (Fig. 1).

The diffusivity of 70 kDa dextran was determined locally, using scanning microphotolysis on a confocal laser scanning microscope (Zeiss LSM 510, Zeiss, Thornwood, NY) with a 100×, 1.3-NA oil immersion lens (25,26). Briefly, using the scanning laser, a line was simultaneously photobleached and imaged, and the diffusion coefficient was computed from a model of the rate of change of fluorescent intensity (26). At each site of diffusion measurement, the distance from the surface of the cartilage was also measured. Dextran at 70 kDa is similar in size to some small matrix components, such as decorin, biglycan, and fibromodulin, and some growth factors such as cartilage-derived growth factor, bone morphogenetic protein-1, and transforming growth factor-β (27,28).

Using the 10× lens, matched images of the full thickness of the cartilage showing the nuclei were taken for strain analysis before and after the tissue was compressed. Tissue was allowed to equilibrate for 30 min after a load was applied, to allow time for all compression-induced fluid flow to cease. After compression, the diffusion measurements were repeated. Nominal tissue-average strain (surface-to-surface strain) was calculated from the distance between the platens, and ranged from 0 to −0.4. Local strain was measured in the tissue, using texture correlation on the images of nuclei (15,29). Texture correlation uses the inherent patterns in an image to track the displacement of regions from the original to the compressed image. Lagrangian strains were calculated from the displacement data. Strains normal for the direction of compression, transverse strains, shear strains, and volumetric strains were calculated. Strains were averaged across the width of the tissue, because the primary variation was with depth in the tissue. Thus, for a given diffusivity measurement at a specific depth, a depth-specific strain was determined. The fractional change in diffusivity was calculated as the difference between depth-matched diffusivity measurements in a compressed and uncompressed sample, divided by the uncompressed diffusivity. Measured displacements were used to map the locations of experiments in compressed tissue onto the corresponding locations in the uncompressed tissue.

Measurement of diffusional anisotropy

Similar experiments were performed to measure the effects of compression on diffusional anisotropy of 70 kDa dextran. Diffusional anisotropy was measured locally, using fluorescence imaging of continuous point photobleaching (FICOPP) experiments (20). Briefly, this technique involves the continuous exposure of a single point in the tissue, using a high-power laser. The fluorescent dextran molecules within this region are photobleached and diffuse away from the point. The bleached region forms an ellipse, where the square of the ratio of the radii of the primary axes of the ellipse is proportional to the ratio of the diffusion coefficients in those directions. The FICOPP experiments were performed at varying distances from the articular surface of the tissue on compressed and uncompressed tissue. As described above, images of nuclei were taken before and after compression to calculate strain, using texture correlation. Diffusional anisotropy was calculated from the FICOPP experiments as the ratio of diffusivity parallel to the surface over diffusivity perpendicular to the surface.

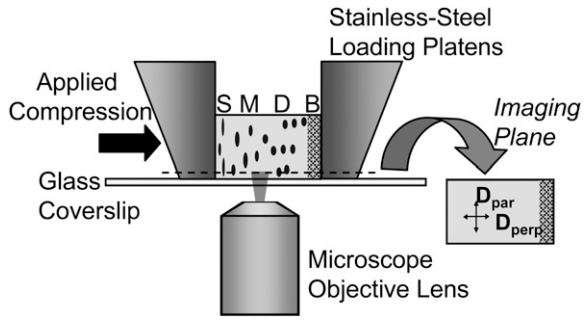

FIGURE 1 Setup for compression-diffusion experiments shows direction of compression and imaging of cartilage explant, which is marked to indicate surface (*S*), middle (*M*), deep (*D*), and bone (*B*) regions. Right side of image shows orientation of anisotropy measurements on tissue in imaging plane.

Analysis

For certain analyses, depth data were grouped by zone, with zones defined in terms of local cell morphology and tissue architecture (30). The surface zone was distinguished by closely packed, elongated cells; the middle zone was distinguished by single, rounded cells; and the deep zone was distinguished by a sparse cell population and radial stacks of rounded cells. For other analyses, the strain data were grouped by magnitude into high-strain (average, −0.29; minimum, −0.21; maximum, −0.38), low-strain (average, −0.12; minimum, −0.04; maximum, −0.20), and zero-strain categories. The term ''strain'' always refers to site-specific Lagrangian strain, and not surface-to-surface tissue-average strain, unless otherwise noted.

The relationship between change in diffusivity and different strain variables was analyzed using linear least-squares regression. Regressions where a particular intercept was deemed to be physically required were fit without an intercept (intercept forced through 0 or 1, as appropriate) (31). One complexity in interpreting the R^2 values from these regressions is the fact that they can be negative (indicating that the mean is a better fit than the regression line), so both R^2 based on variability around the mean (the typically reported value) and R^2 based on variability around the set intercept were also calculated (31,32).

Similarly, anisotropy data were analyzed separately by zone. The relationships between diffusional anisotropy and different strain variables were analyzed using linear least-squares regression. Diffusional anisotropy was log-transformed in these analyses, to meet the assumptions of linear regression. Anisotropy in different strain groupings was also compared using analysis of variance. The presence of significant anisotropy was determined by testing whether the ratio of diffusivities parallel versus perpendicular to the surface was significantly different from 1 (according to paired *t*-test).

RESULTS

Diffusion coefficients

At each level of compression, normal strains were generally highest in the surface zone, and declined toward the middle and deep zones (Fig. 2). The average uncompressed diffusivity was 33 $\mu m^2 s^{-1}$, with diffusivity decreasing to as low as 7 $\mu m^2 s^{-1}$ when the tissue was strained. The fractional change in diffusivity significantly decreased with increasing levels of applied compression (Fig. 3, Table 1). The amount of tissue-average strain was significantly correlated with fractional change in diffusivity, with an R^2 intercept value of 0.51, indicating that tissue-average strain can explain 51% of the variation in fractional change in diffusivity. The site-specific normal strain was also significantly correlated with change in diffusivity. Site-specific normal strain, however, was able to explain much more of the variation in diffusivity (67%) than did tissue-average strain. Dilatation (i.e., volumetric strain) also correlated significantly with fractional change in diffusivity, explaining 64% of the variance. Shear strain did not correlate significantly with fractional change in diffusivity.

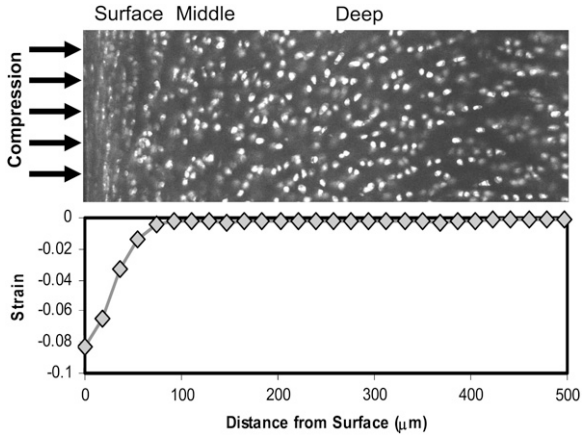

FIGURE 2 Texture correlation analysis of nuclei-labeled images (*above*) yielded site-specific normal-strain profiles through the depth of the tissue (*below*). This image indicates how a given applied strain (7.5%) can yield very different strains from the surface zone (8%) to the middle and deep zones (0%). Deformation of middle and deep zones required application of larger strains.

Although transverse strain had a significant relationship with fractional change in diffusivity, the low R^2 value indicates that it is unable to explain a significant amount of the variability in diffusion. In all cases, the relationship between strain and diffusivity was not dependent on site (i.e., zone).

Diffusional anisotropy

In free-swelling explants (no compression), only the surface zone exhibited significant diffusional anisotropy (Fig. 4). Significant anisotropy was present in the surface zone at all levels of compression, and diffusional anisotropy increased significantly with higher levels of compression. The middle zone only showed significant anisotropy at the highest level of compression (30%). No anisotropy was present in the deep zone, even under the highest strains. Plots of anisotropy versus depth show a rapid rise in anisotropy on the surface of the cartilage, especially at higher strains, as well as a deeper penetration of anisotropy with depth at higher strains (Fig. 5).

The magnitude of diffusional anisotropy generally increased with increasing compression, and was highest on the surface of the tissue, decreasing rapidly with depth. The anisotropy ratio (log-transformed) was significantly correlated with increasing normal strain and volumetric strain in the surface and middle zones (Table 2, Fig. 6). Both normal strain and volumetric strain explained a similar amount of variation in anisotropy. Normal strain explained 31% in the surface zone and 24% in the middle zone, and volumetric strain explained 29% in the surface zone and 22% in the middle zone. The anisotropy ratio (log-transformed) was also significantly correlated with shear strain in the surface zone, and with transverse strain in the middle zone. Anisotropy was not significantly correlated with any strain variables in the deep zone.

DISCUSSION

Our findings indicate that compression of articular cartilage results in localized, zone-specific decreases in diffusivity that correlate more closely with site-specific tissue strains than with nominal surface-to-surface (tissue-average) strains. Both normal strain and volumetric (dilatational) strain explained more of the change in diffusivity than did local shear strains or surface-to-surface strains. Furthermore, compression increased the anisotropy of the diffusion coefficient, particularly in the surface zone of the tissue, increasing the coefficient of diffusion by up to 1.7 times parallel to the surface of the tissue, compared with the perpendicular direction at the highest levels of compression (30%). These findings provide further evidence that the transport properties of articular cartilage are directly coupled to the local state of deformation in tissue (17).

Previous studies, both experimental and theoretical, showed that the decrease in diffusivity associated with compression is a direct function of the fluid volume fraction or proteoglycan content (7,8,21). Because the amount of fluid expressed from tissue with compression is a function of local strain (i.e., dilatation), our results, showing a decrease in diffusivity as a function of strain, support these findings. Furthermore, because the surface zone undergoes much higher local strain for a given amount of surface-to-surface compression, diffusivity in the surface zone is affected to a much greater extent than in the middle or deep zones. For example, for an applied surface-to-surface strain of 30%, the site-specific tissue strain can range from 36% in the surface zone to 12% in the deep

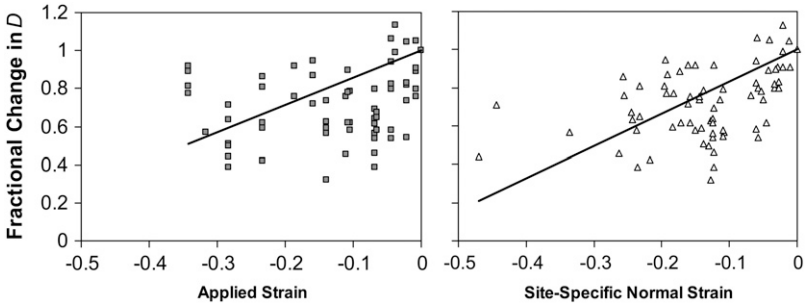

FIGURE 3 Fractional change in diffusivity (D) decreases with increasing compressive strain. Site-specific strain (*right*) explains more variability in the data than does applied strain (*left*). See Table 1 for regression statistics.

TABLE 1 Results of linear least-squares regression of fractional change in diffusion coefficient versus strain variables

	Intercept	Slope	Slope SE	p	R^2 mean	R^2 intercept
Applied strain	1.00	1.43	0.14	0.001	−0.07	0.51
Site-specific strain	1.00	1.68	0.12	<0.0001	0.28	0.67
Volumetric strain	1.00	1.48	0.12	<0.0001	0.20	0.64
Shear strain	1.00	0.56	1.39	0.69	−1.19	0.002
Transverse strain	1.00	4.06	1.60	0.01	−1.05	0.06

For all regressions, $n = 94$ (from 13 animals). Intercepts were specified (not fit). Slope SE, standard error of slope estimate; p, p-value for test of whether slope is significantly different from zero; R^2 mean, variability explained by regression versus that explained by the mean; and R^2 intercept, variability explained by regression versus that explained by intercept.

zone (15). Thus, with compression, dramatic differences may occur in the magnitude and anisotropy of the diffusion coefficient of the surface zone in particular.

We hypothesized that diffusional anisotropy would increase with increasing compression in a zone-dependent manner. In the surface zone, the alignment of collagen fibers parallel to the surface was associated with significant diffusional anisotropy in the free-swelling state, with diffusion occurring faster parallel to the surface, along the fibers, than perpendicular to the surface (20). This anisotropy increased with increasing compression, which presumably packs these fibers closer together. Theoretical models showed that the degree of anisotropy increases rapidly as the fiber volume fraction increases (21,22).

Previous studies showed that proteoglycans clearly affect diffusion rates in cartilage (5,7). Typically, collagen has not been considered a significant influence on the diffusion of molecules in cartilage, because the fibers are relatively large and widely spaced, compared with the proteoglycans (33). The ability of structural molecules to slow the diffusion around them is a function of the size of both the structural and

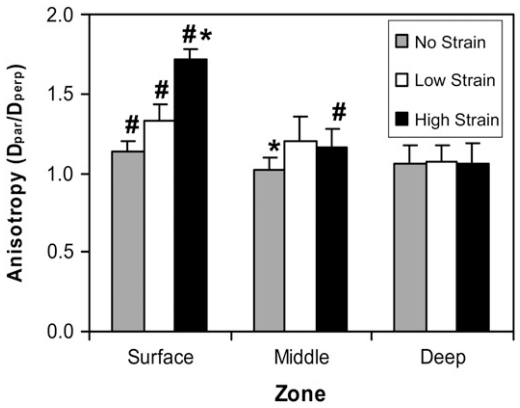

FIGURE 4 Diffusional anisotropy ratio in surface, middle, and deep zones of cartilage for different levels of strain (mean ± SE, $n = 5$–15 per group). (#) Anisotropy is significantly >1 (paired t-test, $p < 0.05$). (*) Mean anisotropy is significantly different from other strain levels in that zone (analysis of variance, $p < 0.05$).

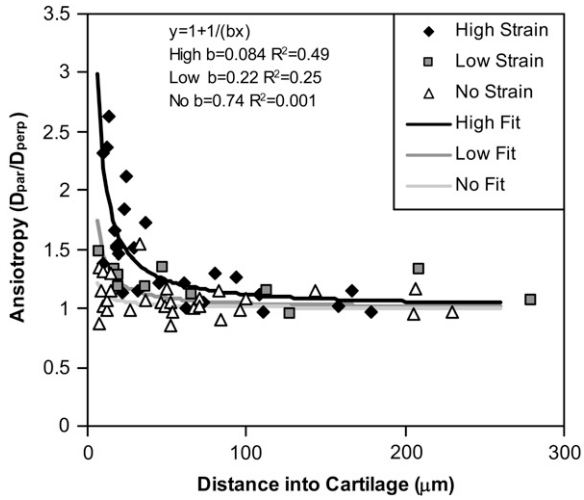

FIGURE 5 Diffusional anisotropy (parallel [D_{par}] versus perpendicular [D_{perp}] to cartilage surface) significantly decreased with increasing depth at all strain levels. Lines show data fits to equation $y = 1 + 1/(bx)$. Coefficients and R^2 values for all fits are shown. All coefficients are significantly different from zero ($p < 0.05$).

the diffusing molecule, and the spacing of the structural molecules. Collagen fibrils in the surface zone are 25–50 nm in diameter, whereas those in the middle and deep zones are 60–160 nm in diameter (34). The volume fraction of collagen fibers in cartilage, however, is ~30% (35). Although the spaces between fibers are larger than 70 kDa dextran, the volume fraction of fibers is sufficiently high that they may still hinder diffusion. Theoretical simulations show that diffusion of a molecule in a solution of fibers of twice the diameter of the diffusing molecule can diffuse up to three times faster parallel to the fibers than perpendicular to the fibers when the fibers are present at a volume fraction of 30%, and this anisotropy will rapidly increase as fiber volume fraction increases, which is what occurs when the tissue is compressed (22). This prediction suggests that the rate of diffusion of many physiologic molecules could be hindered by surface-zone and even middle-zone collagen fibers, if the tissue is significantly compressed.

In the middle zone, collagen fibers are more randomly oriented, but previous work suggests that as the tissue is compressed, these fibers become more aligned (18,19). Our data show the presence of diffusional anisotropy in the middle zone at high strains, suggesting that some degree of collagen orientation is induced by tissue compression. However, no anisotropy was detected in the deep zone in either the free-swelling or compressed states. These findings are consistent with theoretical models of anisotropic diffusion (21) that predict isotropic diffusion properties in the presence of widely spaced (60–100 nm (34)) collagen fibers. Furthermore, because the fibers are aligned perpendicular to the direction of compression, and because the modulus of the deep-zone cartilage is approximately an order of magnitude greater than that of the surface zone (14,15,36), the small magnitudes of local

TABLE 2 Results of linear least-squares regression of ln(anisotropy) versus strain variables for three zones of cartilage

Strain type	Zone	Intercept	SE	p	Slope	SE	p	R^2	n
Normal strain	Surface	0.17	0.06	0.005*	−0.99	0.27	0.0008*	0.31	33
	Middle	0.03	0.03	0.40	−0.42	0.19	0.04*	0.24	18
	Deep	0.07	0.04	0.07	0.03	0.23	0.90	0.001	17
Volumetric strain	Surface	0.18	0.06	0.003*	−0.97	0.27	0.001*	0.29	33
	Middle	0.03	0.03	0.37	−0.42	0.20	0.05*	0.22	18
	Deep	0.07	0.03	0.04*	0.05	0.24	0.83	0.003	17
Transverse strain	Surface	0.29	0.05	0.0001*	5.21	4.56	0.26	0.04	33
	Middle	0.04	0.03	0.17	15.91	5.73	0.01*	0.33	18
	Deep	0.06	0.03	0.04*	0.34	1.39	0.81	0.004	17
Shear strain	Surface	0.26	0.05	0.0001*	−10.69	5.32	0.05*	0.12	33
	Middle	0.06	0.03	0.09	−5.29	5.62	0.36	0.05	18
	Deep	0.07	0.02	0.01*	−0.10	2.14	0.96	0.0001	17

SE, standard error of regression parameter estimate (intercept or slope); p, p-value for test of whether regression parameter is significantly different from zero; *, significant p-value; and n, number of data points in regression.

strains under physiologic loading in the deep zone are unlikely to alter fiber spacing or architecture (37).

The effects of compression on diffusivity were explained equivalently by either local normal strain or dilatation (volumetric strain), but not by transverse or shear strain. Similarly, the amount of diffusional anisotropy in the surface zone was also explained equivalently by normal strain and volumetric strain in the surface zone. These findings are likely attributable to two factors. First, neither the shear nor transverse strain resulted in material consolidation, whereas the dilatation associated with tissue compression resulted in a loss of interstitial fluid and higher local concentrations of proteoglycans and collagen. Second, the magnitudes of shear strain and transverse strains were small compared with the normal strain and dilatation strain, because of the relatively small Poisson's ratio of the tissue (15,38). Therefore, the normal strain dominates the transverse-strain contribution to the volumetric strain. Normal and volumetric strain also explained a considerable amount of the variation in diffusional anisotropy in the middle zone. Transverse strain, however, was the best correlate for anisotropy in the middle zone. This may be attributable to the higher Poisson's ratio in the middle zone relative to the surface zone (14,38–40) and the concomitant lateral expansion of the tissue that increases fiber alignment.

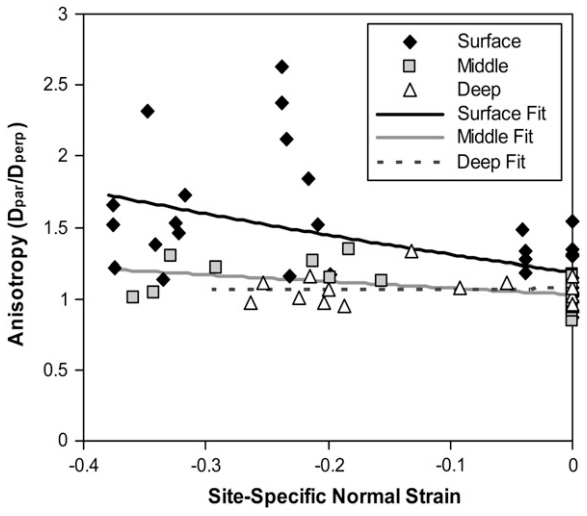

FIGURE 6 Diffusional anisotropy (parallel [D_{par}] versus perpendicular [D_{perp}] to cartilage surface) significantly increases with increasing levels of compressive strain in surface and middle zones, but not in deep zone. See Table 2 for regression statistics.

Compression of cartilage will result in overall decreased diffusivity and decreased diffusivity perpendicular to the surface of the tissue, suggesting that the transport properties of the surface of the tissue may be significantly altered when tissue is compressed, with the net effect of decreasing macromolecular diffusion between the tissue and synovial fluid. Previous studies suggested that physiologic loading may lead to cartilage strains on the order of 5–20%, depending on the activity (41,42). Thus the combined effects of decreased diffusivity and increased anisotropy would make the diffusion time across the surface zone go from ~75 s with no strain, to 89 s with 5% strain in the surface zone, to 208 s with 20% strain in the surface zone. Presumably this effect would be further magnified with larger molecules, and diminished with smaller ones. Degradation or loss of the superficial zone, which may occur with arthritis, could alter this effect, allowing further loss of structural molecules from the cartilage surface. Future studies examining the diffusion properties of biologically relevant molecules, such as proteoglycans or growth factors, in normal and arthritic tissue could shed light on this issue. Furthermore, mimicking these unique, site-specific diffusive properties may be necessary to achieve normal chondrocyte function in tissue-engineered cartilage.

We thank C. L. Gilchrist and L. A. Setton for assistance with the texture correlation analysis, and S. E. Christensen for assistance with the scanning-microphotolysis analysis.

This study was supported by the American Association of University Women and the National Institutes of Health (grants AI07217, AG15768, AR48852, AR50245, and AR48182).

REFERENCES

1. Leddy, H. A., H. A. Awad, and F. Guilak. 2004. Molecular diffusion in tissue-engineered cartilage constructs: effects of scaffold material, time, and culture conditions. *J. Biomed. Mater. Res. B Appl. Biomater.* 70B: 397–406.
2. Maroudas, A. 1970. Distribution and diffusion of solutes in articular cartilage. *Biophys. J.* 10:365–379.
3. Maroudas, A. 1979. Physicochemical properties of articular cartilage. *In* Adult Articular Cartilage. M. A. R. Freeman, editor. Pitman Medical, Bath, UK. 215–290.
4. Torzilli, P. A. 1993. Effects of temperature, concentration and articular surface removal on transient solute diffusion in articular cartilage. *Med. Biol. Eng. Comput.* 31:S93–S98.
5. Torzilli, P. A., J. M. Arduino, J. D. Gregory, and M. Bansal. 1997. Effect of proteoglycan removal on solute mobility in articular cartilage. *J. Biomech.* 30:895–902.
6. Leddy, H. A., and F. Guilak. 2003. Site-specific molecular diffusion in articular cartilage measured using fluorescence recovery after photobleaching. *Ann. Biomed. Eng.* 31:753–760.
7. Evans, R. C., and T. M. Quinn. 2005. Solute diffusivity correlates with mechanical properties and matrix density of compressed articular cartilage. *Arch. Biochem. Biophys.* 442:1–10.
8. Nimer, E., R. Schneiderman, and A. Maroudas. 2003. Diffusion and partition of solutes in cartilage under static load. *Biophys. Chem.* 106: 125–146.
9. Quinn, T. M., P. Kocian, and J. J. Meister. 2000. Static compression is associated with decreased diffusivity of dextrans in cartilage explants. *Biophys. Chem.* 384:327–334.
10. Buschmann, M. D., Y. A. Gluzband, A. J. Grodzinsky, and E. B. Hunziker. 1995. Mechanical compression modulates matrix biosynthesis in chondrocyte/agarose culture. *J. Cell Sci.* 108:1497–1508.
11. Guilak, F., B. C. Meyer, A. Ratcliffe, and V. C. Mow. 1994. The effects of matrix compression on proteoglycan metabolism in articular cartilage explants. *Osteoarthritis Cartilage.* 2:91–101.
12. Gray, M. L., A. M. Pizzanelli, A. J. Grodzinsky, and R. C. Lee. 1988. Mechanical and physiochemical determinants of the chondrocyte biosynthetic response. *J. Orthop. Res.* 6:777–792.
13. Chen, A. C., W. C. Bae, R. M. Schinagl, and R. L. Sah. 2001. Depth- and strain-dependent mechanical and electromechanical properties of full-thickness bovine articular cartilage in confined compression. *J. Biomech.* 34:1–12.
14. Wang, C., J. Deng, G. Ateshian, and C. Hung. 2002. An automated approach for direct measurement of two-dimensional strain distributions within articular cartilage under unconfined compression. *J. Biomech. Eng.* 124:557–567.
15. Choi, J. B., I. Youn, L. Cao, H. A. Leddy, C. L. Gilchrist, L. A. Setton, and F. Guilak. 2007. Zonal changes in the three-dimensional morphology of the chondron in articular cartilage under compression: the relationship between cellular, pericellular, and extracellular deformation. *J. Biomech.* 40:2596–2603.
16. Quinn, T. M., P. Dierickx, and A. J. Grodzinsky. 2001. Glycosaminoglycan network geometry may contribute to anisotropic hydraulic permeability in cartilage under compression. *J. Biomech.* 34:1483–1490.
17. Reynaud, B., and T. M. Quinn. 2006. Anisotropic hydraulic permeability in compressed articular cartilage. *J. Biomech.* 39:131–137.
18. Alhadlaq, H. A., and Y. Xia. 2004. The structural adaptations in compressed articular cartilage by microscopic MRI ([mu]MRI) T2 anisotropy. *Osteoarthritis Cartilage.* 12:887–894.
19. Kääb, M. J., K. Ito, J. M. Clark, and H. P. Nötzli. 1998. Deformation of articular cartilage collagen structure under static and cyclic loading. *J. Orthop. Res.* 16:743–751.
20. Leddy, H. A., M. A. Haider, and F. Guilak. 2006. Diffusional anisotropy in collagenous tissues: fluorescence imaging of continuous point photobleaching. *Biophys. J.* 91:311–316.
21. Han, J., and J. Herzfeld. 1993. Macromolecular diffusion in crowded solutions. *Biophys. J.* 65:1155–1161.
22. Lubkin, S. R., and X. Wan. 2006. Optimizing detection of tissue anisotropy by fluorescence recovery after photobleaching. *Bull. Math. Biol.* 68:1873–1891.
23. Guilak, F. 1995. Compression-induced changes in the shape and volume of the chondrocyte nucleus. *J. Biomech.* 28:1529–1541.
24. Guilak, F., A. Ratcliffe, and V. C. Mow. 1995. Chondrocyte deformation and local tissue strain in articular cartilage: a confocal microscopy study. *J. Orthop. Res.* 13:410–421.
25. Kubitscheck, U., P. Wedekind, and R. Peters. 1998. Three-dimensional diffusion measurements by scanning microphotolysis. *J. Microsc.* 192: 126–138.
26. Leddy, H. A., S. E. Christensen, and F. Guilak. Microscale diffusion properties of the cartilage pericellular matrix measured using 3D scanning microphotolysis. *J. Biomech. Eng.* In press.
27. Heinegard, D., and A. Oldberg. 1989. Structure and biology of cartilage and bone matrix noncollagenous macromolecules. *FASEB J.* 3: 2042–2051.
28. Seyedin, S. M., and D. M. Rosen. 1991. Cartilage growth and differentiation factors. *In* Cartilage: Molecular Aspects. B. Hall and S. Newman, editors. CRC Press, Boston. 131–151.
29. Gilchrist, C., J. Xia, L. Setton, and E. Hsu. 2004. High-resolution determination of soft tissue deformations using MRI and first-order texture correlation. *IEEE Trans. Med. Imaging.* 23:546–553.
30. Eggli, P. S., E. B. Hunziker, and R. K. Schenk. 1988. Quantitation of structural features characterizing weight- and less-weight-bearing regions in articular cartilage: a stereological analysis of medial femoral condyles in young adult rabbits. *Anat. Rec.* 222:217–227.
31. Eisenhauer, J. G. 2003. Regression through the origin. *Teach. Stat.* 25: 76–80.
32. Kvalseth, T. O. 1985. Cautionary note about R^2. *Am. Stat.* 39:279–285.
33. Maroudas, A. 1975. Biophysical chemistry of cartilaginous tissues with special reference to solute and fluid transport. *Biorheology.* 12:233–248.
34. Hwang, W. S., B. Li, L. H. Jin, K. Ngo, N. S. Schachar, and G. N. Hughes. 1992. Collagen fibril structure of normal, aging, and osteoarthritic cartilage. *J. Pathol.* 167:425–433.
35. Langsjo, T. K., M. Hyttinen, A. Pelttari, K. Kiraly, J. Arokoski, and H. J. Helminen. 1999. Electron microscopic stereological study of collagen fibrils in bovine articular cartilage: volume and surface densities are best obtained indirectly (from length densities and diameters) using isotropic uniform random sampling. *J. Anat.* 195:281–293.
36. Schinagl, R. M., D. Gurskis, A. C. Chen, and R. L. Sah. 1997. Depth-dependent confined compression modulus of full-thickness bovine articular cartilage. *J. Orthop. Res.* 15:499–506.
37. Alhadlaq, H. A., and Y. Xia. 2005. Modifications of orientational dependence of microscopic magnetic resonance imaging T2 anisotropy in compressed articular cartilage. *J. Magn. Reson. Imaging.* 22:665–673.
38. Jurvelin, J., M. Buschmann, and E. Hunziker. 2003. Mechanical anisotropy of the human knee articular cartilage in compression. *Proc. Inst. Mech. Eng. [H].* 217:215–219.
39. Jurvelin, J. S., M. D. Buschmann, and E. B. Hunziker. 1997. Optical and mechanical determination of Poisson's ratio of adult bovine humeral articular cartilage. *J. Biomech.* 30:235–241.
40. Laasanen, M. S., J. Töyräs, R. K. Korhonen, J. Rieppo, S. Saarakkala, M. T. Nieminen, J. Hirvonen, and J. S. Jurvelin. 2003. Biomechanical properties of knee articular cartilage. *Biorheology.* 40:133–140.
41. Armstrong, C., A. Bahrani, and D. Gardner. 1979. In vitro measurement of articular cartilage deformations in the intact human hip joint under load. *J. Bone Joint Surg. [Am.]* 61:744–755.
42. Eckstein, F., B. Lemberger, T. Stammberger, K. H. Englmeier, and M. Reiser. 2000. Patellar cartilage deformation in vivo after static versus dynamic loading. *J. Biomech.* 33:819–825.